Evidence of electronic growth in titanium- and cobalt-silicide islands

S. Manor · J. K. Tripathi · I. Goldfarb

Abstract A possibility of growing highly mismatched and yet two-dimensional heteroepitaxial deposits, is both fascinating in terms of basic science and technologically important. So far, stabilization of flat morphology by a reduction of the overall electron energy in a quantum well (hence termed "electronic growth"), has been observed exclusively in heteroepitaxy of simple metals, lead, and silver. This work shows, that a broader class of functional materials can be grown "electronically," such as titanium- and cobalt-silicide nano-islands on Si(111), despite their more complex electronic structure.

Introduction

Itinerant electrons in ultra-thin (<de Broglie wavelength) films are one-dimensionally (1D) confined by the lower and upper interfaces, and bounce between them, producing a quantum well (QW) with discrete energy states or QW sub-bands (QWS's) [1]. In an infinite potential well, these are bound states represented by standing waves having nodes at the walls of the well, whose wavelengths are given by the interference condition imposed on the QW thickness (H), which must contain integer number (quantum number, n) of half the wavelengths, $H = Nd_{(hkl)} = n\lambda_n/2$, where the film thickness H comprised of N atomic (hkl)-planes ($d_{(hkl)}$

S. Manor · J. K. Tripathi · I. Goldfarb (✉)
School of Mechanical Engineering and Materials
& Nanotechnologies Program, Faculty of Engineering,
Tel Aviv University, Ramat Aviv, 69978 Tel Aviv, Israel
e-mail: ilang@eng.tau.ac.il

I. Goldfarb
Research Center for Nanoscience and Nanotechnology,
Tel Aviv University, Ramat Aviv, 69978 Tel Aviv, Israel

being interplanar distance) [2]. No occupied states exist above Fermi energy (E_F), hence the highest occupied state (HOS) may reside at the Fermi level, but not above it. As the thickness of the QW increases, more states (higher n) will be introduced, until, in the bulk limit, they form an almost undistinguishable continuum. However, in the process of thickening, Fermi level crossing by the increasing number of newly formed QWS's will take place, such that new occupied sub-bands will start dropping below the Fermi surface in a sequential manner [3–7]. This also means that, since QWS's pass through the Fermi surface upon thickening, there must exist thicknesses corresponding to a formation of QWS's exactly, or very close to the Fermi level. Such a full or even partial overlap between these states and the Fermi level raises the QW density of states (DOS), its overall electron energy, destabilizing the film of these thicknesses relative to those whose HOS lie the farthest from the Fermi level [3–6, 8]. A rigorous procedure for finding such thicknesses must consider a realistic well with finite barriers at the interface with vacuum and, in particular, with the substrate due to charge spilling, using Bohr–Sommerfeld phase-accumulation model [9–11]. However, even plain interference conditions for a standing wave in an infinite well reproduce surprisingly well the experimental results, provided the thin metallic QW film is of a simple free-electronlike character [12]. A periodicity of QWS passage through the Fermi level can be found by substituting $n = n_F$, such that $\lambda_n = \lambda_F$, or, expressing the quantization rule via the wave vector, such that $k_n = k_F$, i.e., $H = n_F\pi/k_F$. In the case of lead, in addition to its free-electronlike character in the bulk, simple, almost commensurate relations exist between its (111) periodicity [$d_{(111)} = 2.86$ Å] and the Fermi wavelength ($\lambda_F = 3.66$ Å), such that $d_{(111)} \approx (\frac{3}{4})\lambda_F$, and thus $2d_{(111)} \approx 3(\lambda_F/2)$. This leads to a (111)-bilayer

periodicity of oscillations [13–15], with some experimental results indicating the energetic preference for an odd-layer morphology, e.g., high stability of 5 monolayer (ML) and 7 ML islands as opposed to 6 ML islands [3, 14, 16], while others report just the opposite [6]. The explanation of this apparent discrepancy most likely lies in the slightly different substrate conditions and the strength of the resulting substrate barrier; Ricci et al. [17] have convincingly demonstrated even-to-odd phase shift by interfacial engineering. In addition, since the wavelength commensuracy is not perfect, the phase matching is gradually lost, leading to an odd–even–odd sequence reversal every 7 [16] or 9 [8] MLs. However, regardless of the odd (even) sequence, the intervening even (odd) morphology always yields a maximum in DOS at the Fermi level and in the total electronic energy, thus becoming unstable [13–15] and phase-separating to the next allowed thicknesses above and below [11].

Unsurprisingly, the vast majority of the results in this area have been obtained with lead, e.g., Pb/Si(111) [9, 12–14, 18, 19], Pb/Ge(111) [18], Pb/Cu(111) [10, 15] and silver, e.g., Ag/Si(111) [19, 20], Ag/GaAs(110) [21], and Ag/Fe(100) [11]. Both metals are inert to these substrates, creating sharp uniform interfaces, and their electron states near the Fermi level are of almost free-electronlike *sp* character, allowing a simple prediction of the allowed heights and assignment of quantum numbers to the QWS's [14]. However, since (unlike in lead) there are no simple relations between the Fermi wavelength and the interplanar spacing in silver, no clear oscillations exist, and minimum-energy height(s) has to be found by taking potential-lowering due to charge spilling into account [1, 22]. Finally, it is noteworthy that the electronic growth opposes the more familiar Stranski–Krastanow (SK) or Vollmer–Weber (VW) growth modes, governed by competition between the elastic and the surface and interface energies. Therefore, the concept of "critical thickness" has the opposite to the SK meaning, namely the thickness of 3D-to-2D transition.

This work shows, that electronic growth of flat fixed-height islands and layers need not be limited to simple metals, and its signature of a QW-like DOS and "magic heights" emerge in far more complex $TiSi_2/Si(111)$ and $CoSi_2/Si(111)$ heterosystems. Judging from their uniform flat-topped appearance (cf. Ref [23, 24]), possibly other transition-metal silicides grow electronically, indicating a much broader phenomenon.

Experimental

The experiments were performed in an ultra-high vacuum (UHV, base pressure 1×10^{-10} mbar) variable-temperature scanning tunneling microscope (VT-STM) with low- (LEED) and reflection high-energy electron diffraction

(RHEED) and Auger spectrometer. Samples cut from singular and 4°-miscut vicinal Si(111) [hereafter vicSi(111)] wafers were degreased, and in the UHV degassed, flashed at 1,150–1,200 °C, and cooled to room temperature (RT), at which point well ordered (7 × 7) pattern appeared both in diffraction and STM images. Ti and Co were evaporated at RT onto vicinal and singular samples mounted at the VT-STM stage, until the complete "burial" of a (7 × 7) reconstruction beneath a uniform and dense coverage of non-reacted metal clusters and replacement of a (7 × 7) diffraction pattern by a bulk-terminated (1 × 1). Consequently, all four specimens, *Ti/Si(111)*, *Ti/vicSi(111)*, *Co/Si(111)*, and *Co/vicSi(111)*, underwent a series of annealing treatments up to 700 °C under continuous constant-current STM imaging. All the images were acquired using $I = 0.1$–0.2 nA and -3.0 V $< V < +3.0$ V tunneling conditions and shown in the (current) *I*-mode. Single-point scanning tunneling spectroscopy (STS) was used to collect *I–V* spectra at RT, by placing the tip above an island, momentarily disconnecting the feedback loop, and ramping the voltage from -3 to $+3$ V. Tunneling conductance spectra, d*I*/d*V* vs. *V*, were obtained by numerical differentiation of the *I–V* curves.

Results and discussion

Titanium-silicide islands

Figure 1 shows shape evolution of titanium-silicide islands with temperature on a singular Si(111) substrate, with the STM images characteristic of each temperature on the left, and plot of the island heights as a function of widths on the right (with height distributions in the insets). In all four specimens, no significant redistribution of the deposited metal took place below ~ 500 °C, where apparently Me–Si reaction and formation of the first silicide islands normally begins. In the Ti/Si(111) case, most of the broadly distributed conical silicide islands at 500–600 °C, shown in Fig. 1a, had heights in the 0.5–1.0 nm range, with only a few 1.5–2 nm tall (see inset), with the island heights growing simultaneously with their widths (as expected in a 3D growth). However, already at 650 °C (Fig. 1b), there were more than 10% of tall islands at the expense of the smaller ones, with the most probable height of about 2.1 nm. It follows from the height versus diameter plot, that once the islands reach that height, they stop growing upwardly and only keep extending laterally, indicating the onset of a 3D-to-2D transition. This trend gets even more pronounced at 700 °C, as shown in Fig. 1c. The trend of discrete conical islands that coarsen until they reach about 2.1 nm height, and then undergo 3D-to-2D shape transition by apex truncation, was also evident in the Ti/vicSi(111) sample shown in Fig. 2, despite somewhat higher island
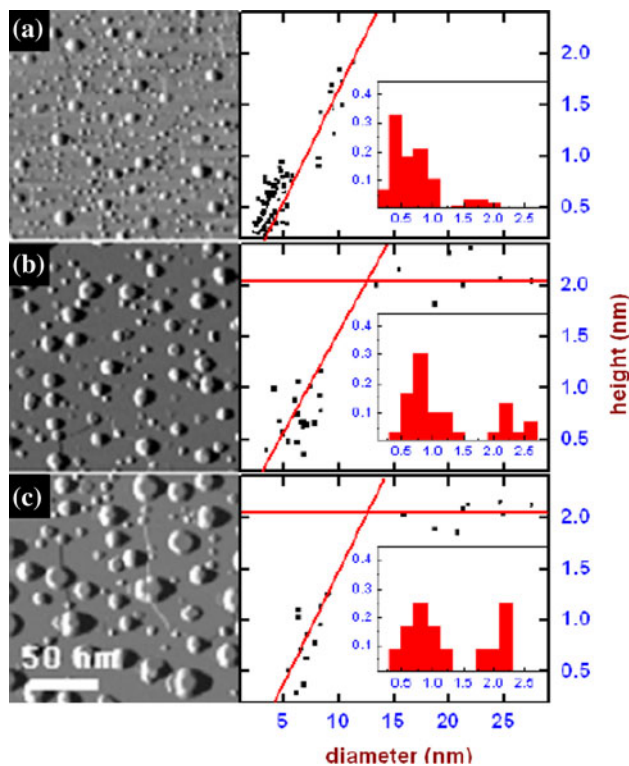
Fig. 1 **a–c** Temperature-dependent STM images of the TiSi$_2$/Si(111) islands (*left hand side*), and their size–shape evolution expressed as height versus diameter plot (*right hand side*). In the *insets*: island height distribution expressed as probability (*vertical axis*) of finding island of certain height (nm, *horizontal axis*). **a** 500 °C anneal, **b** 650 °C anneal, and **c** 700 °C anneal

Fig. 2 **a–c** Temperature-dependent STM images of the TiSi$_2$/vicinal Si(111) islands (*left hand side*), and their height versus diameter plot (*right hand side*). **a** 550 °C anneal, **b** 600 °C anneal, and **c** 650 °C anneal

density. The observed single preferred height of TiSi$_2$ islands (irrespective of the Si(111) surface morphology) resembles the case of Ag, rather than the periodic heights of Pb islands.

Cobalt-silicide islands

Co-covered singular Si(111) surfaces undergo a qualitatively similar evolution, with the most essential stages captured in Fig. 3, i.e., formation and broad distribution of the cobalt-silicide islands at 500 °C, Ostwald ripening of the largest at the expense of the smaller ones at higher temperatures, 3D-to-2D transition, and the formation of preferred "magic" heights. The height distribution plots on the right-hand side of Figs. 3 and 4 belong to the tallest truncated islands (with the tiny ones ignored) and shown in equivalent CoSi$_2$(111) bi-layers (BLs), i.e., $d_{(111)} =$ 0.31 nm, since we are confident that the flat top facets of these islands are CoSi$_2$(111) [25]. In Fig. 3a, truncation of the tallest islands can already be observed at 500 °C. At 600 °C, these truncated islands grow by destabilizing and consuming their smaller neighbors, judging from the large denuded zones around them in Fig. 3b, defining the mean
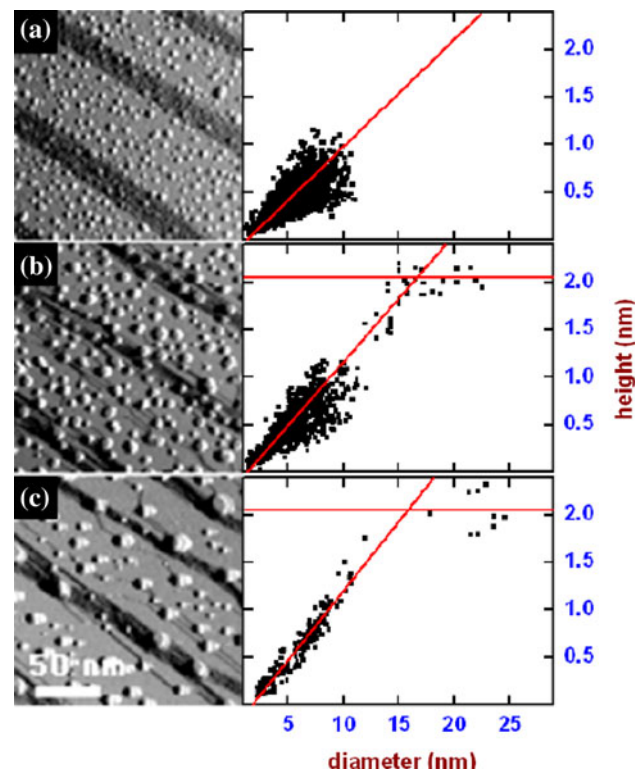
30–40 nm interaction range. Their heights at 600 °C were distributed between two characteristic mean heights (Fig. 3b): 15 BLs (majority) and 17 BLs (minority), with the distribution reversed at 650 °C, i.e., almost no 15 BL-height islands left (Fig. 3c). Unlike the case of titanium-silicide islands, a profound difference was revealed between cobalt-silicide islands grown on singular Si(111) and those on the vicinal Si(111). On singular Si(111), they evolved into compact islands shown in Fig. 3, whereas on vicinal Si(111) the silicide growth was clearly dominated by coalescence, which explains the irregular island shapes extending tens and even hundreds of nanometers laterally with only small gaps between them, creating the appearance of a quasi-continuous film (Fig. 4a, b). This film breaks into taller and more compact islands upon annealing, with the most probable height of 4 BLs at 470 °C (Fig. 4a), 7 BLs at 580 °C (Fig. 4b), and 11–12 BLs at 680 °C (Fig. 4c). Thus, the thickening is not layer-by-layer continuous, but proceeds by discrete jumps to only certain allowed levels. In spite of such a different morphology, the period of the stable height oscillations appears to be similar in CoSi$_2$ islands on both types of the Si(111) surface: 3–4 BLs jumps (this time resembling the behavior of Pb, rather than that of Ag).
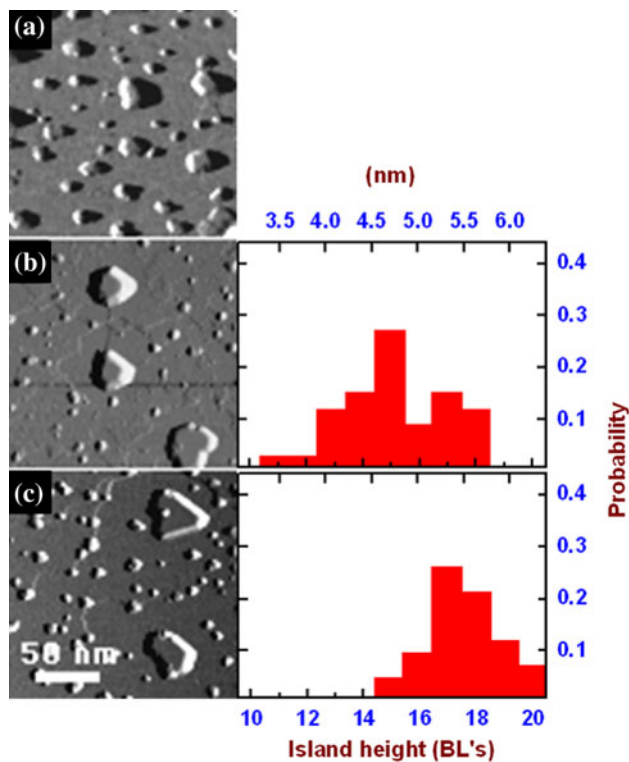
Fig. 3 a–c Temperature-dependent STM images of the CoSi$_2$/ Si(111) islands (*left hand side*), and their height distribution expressed as probability (*vertical axis*) of finding island of certain height (number of equivalent BLs, *horizontal axis*). **a** 500 °C anneal, **b** 600 °C anneal, and **c** 650 °C anneal

Scanning tunneling spectroscopy

In our previous work, we proposed a classical approach to the 3D-to-2D shape transition of TiSi$_2$ nanoislands on Si(111), based on generalized Wulff–Kaishew theorem of equilibrium crystal shapes [26], which may account for sharpening of the growing strained islands with size [27, 28], and flattening [29, 30] upon strain relaxation due to intermixing or strain-relieving defects [26, 31, 32]. Indeed, some of the electronic growth symptoms can be accounted for by classical effects alone or by a competition between classical and quantum-size (QS) effects [33, 34]. Su et al. [19] have noted that electronic growth can be manifested via single-height islands, as in the case of Ag/Si(111) (and Co/vicSi(111) here), or multiple-height islands due to initial 3D growth, as in the case of Pb/Si(111) (and Ti/ Si(111), Ti/vicSi(111), and Co/Si(111) here), with different 3D-to-2D transition pathways and timings for different-height islands.

Unlike Ag/Si(111), Pb/Si(111), and TiSi$_2$/Si(111), CoSi$_2$ is not a priori expected to grow in a 3D fashion on silicon, especially not on Si(111), due to favorable matching conditions. Therefore, in this case, the only way to distinguish classical from QS effects, is to probe the islands' DOS.
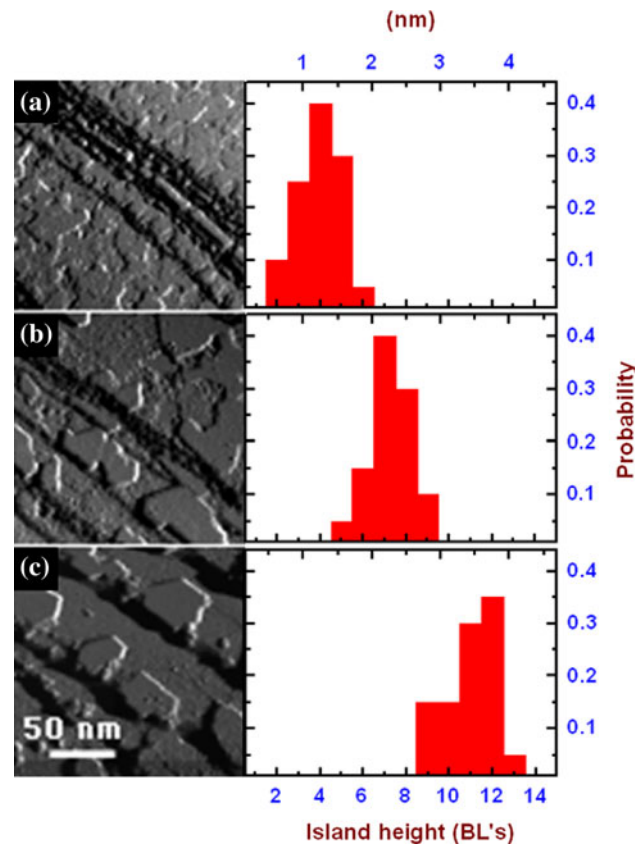

Fig. 4 a–c Temperature-dependent STM images of the CoSi$_2$/vicinal Si(111) islands (*left hand side*), and their height distribution expressed as probability (*vertical axis*) of finding island of certain height (number of equivalent BLs, *horizontal axis*). **a** 470 °C anneal, **b** 580 °C anneal, and **c** 680 °C anneal

Since the electronic wave functions in QW islands are modified by the imposed boundary conditions, the corresponding stepwise increase of DOS with the energy should be readily accessible with STS [13–15]. Figure 5a shows a typical STM image of CoSi$_2$ islands on a *vicinal* Si (111) surface, recorded at RT, and Fig. 5b shows *I–V* curve from the marked island (shown to be flat by a plot profile in the inset). Figure 5c shows a series of typical d*I*/d*V* vs. *V* spectra (proportional to DOS) characteristic of the islands on this surface. Figures 5d–f show the same features, respectively, however of the CoSi$_2$ islands on *singular* Si(111). The vertical solid lines in the center of Fig. 5c, f indicate the position of the Fermi level, small arrows indicate the onsets of the highest occupied (HOS) and lowest unoccupied (LUS) QWS's, and short dotted lines mark the mid position of the quasi-particle HOS–LUS gap (Δ). Generally, for conduction (valence) band to appear at positive (negative) sample bias, and for the bound states in the tunneling spectra to correspond directly to the QWS's, the tip should be sufficiently retracted [35, 36]. This ensures the largest voltage drop on the tip–QW (rather than
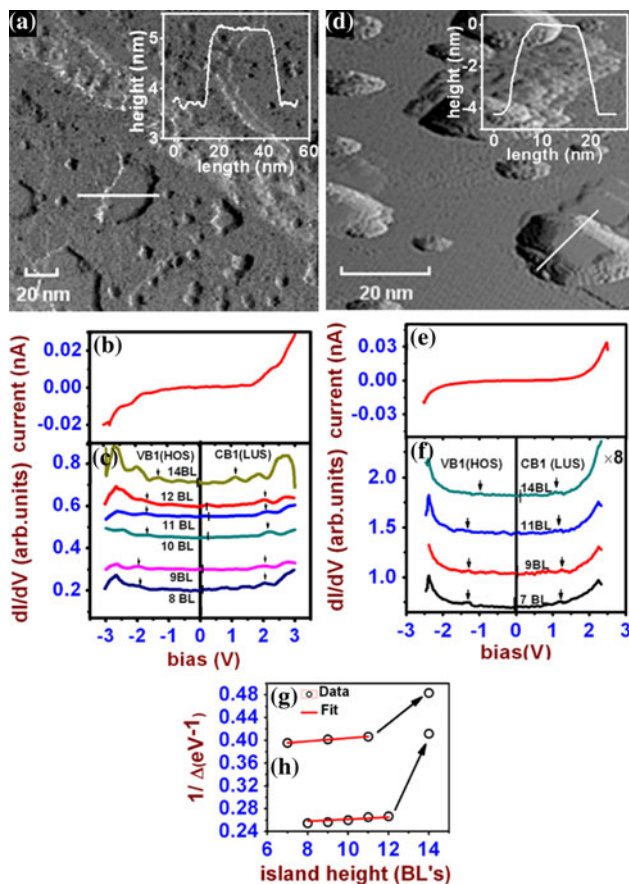
Fig. 5 a–c Electronic structure of CoSi$_2$/vicinal Si(111) islands and **d–f** CoSi$_2$/Si(111) islands at RT, and their respective (**h**) and (**g**) reciprocal LUS–HOS gap dependence on the island height. **a** −3 V and **d** −2.5 V STM images, with island height profiles measured along the indicated white lines in the *insets*, **b** and **e** typical *I–V* curves, and **c–f** characteristic conductance spectra from islands of various heights (7 BLs–14 BLs). Note, that for clarity, d*I*/d*V* intensity in (**f**) is multiplied by 8

QW–substrate) junction and minimization of the single-electron charging effects (that may distort the true electronic structure). However, at RT electron charging may be safely neglected, since the islands in this work are larger than the largest estimated to allow for the charging energy to overcome the thermal energy [37]. It should be stated, that most of the STS spectra were (quite naturally) acquired from the best-defined islands on both types of a surface. In other words, not all the islands counted in the distributions of Figs. 3 and 4 were probed by STS (e.g., ill-defined islands during the initial stages of formation at 470 °C on a vicinal surface, as in Fig. 4a) and, on the other hand, some spectra were acquired from non-typical (minority) islands (e.g., from 7 BLs, 9 BLs, and 11 BLs islands on a singular surface, as shown in Fig. 5f).

The electronic structure difference between the two types of CoSi$_2$ islands, i.e., on vicinal and singular surface, is striking! The *I–V* curves of the islands on a *singular*

surface are quite smooth, resulting in a similarly smooth, "U"-shaped, conductance spectra, with only two tiny bumps indicating the HOS and the LUS. Contrary to that, the islands on the *vicinal* surface exhibit stepped *I–V* curves and periodically peaked DOS, with up to three explicit QWS's in the valence (VB) and conduction band (CB). Moreover, though the QW Δ-gaps are expected to shrink with thickness, the absolute gap values of the same height islands on these two surfaces differ, as well as the magnitude of the reduction: on a vicinal surface the Δ reduces from 3.93 eV at 7 BL islands to 2.43 eV at those of 14 BL-height (Fig. 5c), whereas on the singular surface the corresponding values are 2.53 and 2.07 eV (Fig. 5f), respectively. Plotting the reciprocal gap values as a function of thickness is instrumental for extracting the Fermi velocity (v_F), since the latter defines the slope of the 1/Δ vs. *H* plot, as in $\frac{1}{\Delta} = \frac{(2/h)}{v_F}H$, where *h* is Plank's constant [13, 14]. The so-obtained Fermi velocities for the silicide islands on vicinal and singular Si(111) are 2.81×10^8 m/s (Fig. 5h) and 1.72×10^8 m/s (Fig. 5g), respectively. On the other hand, once the island heightens to 14 BLs, sharp reduction of its Δ occurs regardless of the substrate type, though to different respective values (arrowed in Figs. 5g, h). This most likely indicates the onset of transition from quantum regime to bulk-dominated behavior. Most importantly, for any island height shown in Fig. 5c, f, including the most probable in the distributions of Figs. 3 and 4, the VB1 and CB1 QWS's adjacent to the E_F on both sides, are very distant from it (the mid gap positions, marked by short dotted lines, are either in the very near vicinity or exactly at the Fermi level)—indicating electronic stabilization!

Conclusions

In conclusion, TiSi$_2$ and CoSi$_2$ islands on Si(111) surfaces behave consistently with the so-called "electronic growth" model, by transforming from 3D structures to 2D QWs of only certain allowed thicknesses ("magic heights"). TiSi$_2$ islands grew three-dimensionally in a compact form, up to a height of about 2.1 nm, at which point vertical growth became inhibited, and the islands kept extending only laterally. The morphological evolution and the electronic structure of the CoSi$_2$ islands on a singular surface differed from those on the vicinal one, though both according to the electronic growth model. On a singular surface, the truncated islands coarsened by Ostwald ripening in a compact form, and exhibited magic heights (although with somewhat broad-looking distribution due to their low number density of 2–3 islands per 40,000 nm^2!) and smooth *I–V* curves that, upon numerical differentiation, transformed into U-shaped conductance tunneling spectra. On the

vicinal surface, the islands coalesced to form quasi-continuous layers of magic heights and stepwise increase of tunneling current with the bias. Therefore, their DOS contained QW states in the valence and conduction bands. On both surfaces, the island reciprocal energy gap scaled linearly with the island thickness, confirming the formation of a QW, without, however, overlaps between QW states and the Fermi level for all the islands considered. This indicates stabilization of the abandoned island heights by the electron energy, and low count for those of the higher (due to the overlap) energy, and proves that not only simple metals, but technologically important $TiSi_2/Si(111)$ and $CoSi_2/Si(111)$ (and perhaps more transition-metal silicides and other materials), can be grown two-dimensionally due to electronic stabilization.

It is difficult to account for the electronic structure difference between the $CoSi_2$ islands on singular and vicinal Si(111) without knowing their band structure and details of the Fermi surface (e.g., from density functional theory), which is not, at present, available. It may be the result of the different morphological evolution shown (compact faceted on singular versus irregular non-faceted on vicinal surfaces), or different interface quality. The latter seems the most likely reason: we have managed to find an island on a singular surface that exhibits QWS peaks, similar to

those from the vicinal surface islands, as shown in Fig. 6. Since its shape is not different from the neighbor islands, the immediate suspect must be its individual interface (barrier strength) with the substrate. Su et al. [19] have already noted the dramatic effect of the individual interface formation even on the evolution of neighboring islands on the same surface! While difficult to see in the figures, the singular Si(111) surface between the $CoSi_2$ islands exhibits (7×7) reconstruction, whereas the vicinal surface does not. The most likely explanation is that there is still some free cobalt left between the vicinal surface islands. As mentioned above, this may have a profound effect on the electronic structure of the islands [17]. Summarizing, all the essential indicators of the electronic growth were demonstrated to exist in these silicide islands.

Fig. 6 a A "renegade" $CoSi_2/singular$ Si(111) island exhibiting STS **b** I–V curve and **c** DOS electronic structure (QWS peaks) typical of the islands on a vicinal surface. Note the STM image in (**a**) is a gradient (surface slope) image, where the darker segments indicate higher inclination. The image shows (i) the faceted nature of the islands, and (ii) their flat tops parallel to the substrate plane

References

1. Zhang Z, Niu Q, Shih C-K (1998) Phys Rev Lett 80:5381
2. Milun M, Pervan P, Woodruff DP (2002) Rep Prog Phys 65:99
3. Tringides MC, Jatochowski MJ, Bauer E (2007) Phys Today 60:50
4. Binggeli N, Altarelli M (2006) Phys Rev Lett 96:036805
5. Man KL, Qiu ZQ, Altman MS (2004) Phys Rev Lett 93:236104
6. Upton MH, Wei CM, Chou MY, Miller T, Chiang T-C (2004) Phys Rev Lett 93:026802
7. Mathias S, Wiesenmayer M, Aeschlimann M, Bauer M (2006) Phys Rev Lett 97:236809
8. Zhang Y-F, Jia J-F, Han T-Z, Tang Z, Shen QT, Guo Y, Qiu ZQ, Q-K Xue (2005) Phys Rev Lett 95:096802
9. Mans A, Dil JH, Ettema ARHF, Weitering HH (2002) Phys Rev B 66:195410
10. Otero R, Vázquez de Parga AL, Miranda R (2000) Surf Sci 447:143
11. Luh D-A, Miller T, Paggel JJ, Chou MY, Chiang T-C (2001) Science 292:1131
12. Czoschke P, Hong H, Basile L, Chiang T-C (2004) Phys Rev Lett 93:036103
13. Altfeder IB, Matveev KA, Chen DM (1997) Phys Rev Lett 78:2815
14. Su WB, Chang SH, Jian WB, Chang CS, Chen LJ, Tsong TT (2001) Phys Rev Lett 86:5116
15. Otero R, Vázquez de Parga AL, Miranda R (2002) Phys Rev B 66:115401
16. Eom D, Qin S, Chou M-Y, Shih CK (2006) Phys Rev Lett 96:027005
17. Ricci DA, Miller T, Chiang T-C (2005) Phys Rev Lett 95:266101
18. Özer MM, Jia Y, Wu B, Zhang Z, Weitering HH (2005) Phys Rev B 72:113409
19. Su WB, Lin HY, Chiu YP, Shih HT, Fu TY, Chen YW, Chang CS, Tsong TT (2005) Phys Rev B 71:073304
20. Gavioli L, Kimberlin KR, Tringides MC, Wendelken JF, Zhang Z (1999) Phys Rev Lett 82:129
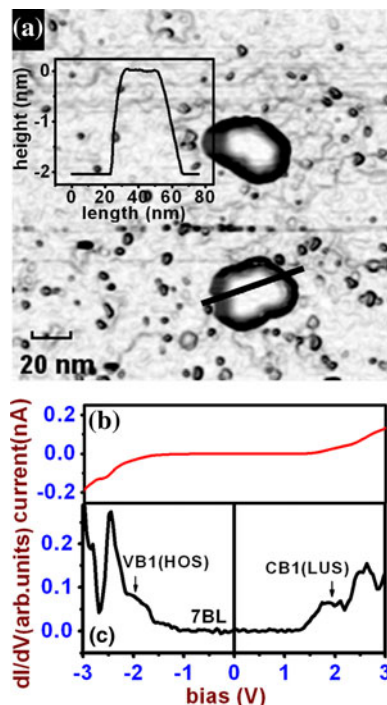21. Yu H, Jiang CS, Ebert Ph, Wang XD, White JM, Niu Q, Zhang Z, Shih CK (2002) Phys Rev Lett 88:016102

22. Hirayama H (2009) Surf Sci 603:1492
23. Wawro A, Suto S, Czajka R, Kasuya A (2003) Phys Rev B 67:195401
24. Azatyan SG, Iwami M, Lifshits VG (2005) Surf Sci 589:106
25. Goldfarb I (2007) Nanotechnology 18:335304
26. Goldfarb I, Cohen-Taguri G, Grossman S, Levinshtein M (2005) Phys Rev B 72:075430
27. Medeiros-Ribeiro G, Bratkovski AM, Kamins TI, Ohlberg DAA, Williams RS (1998) Science 279:353
28. Costantini G, Rastelli A, Manzano C, Songmuang R, Schmidt OG, Kern K, von Känel H (2004) Appl Phys Lett 85:5673
29. Rastelli A, Kummer M, von Känel H (2001) Phys Rev Lett 87:256101
30. Stoffel M, Kar GS, Denker U, Rastelli A, Sigg H, Schmidt OG (2004) Physica E 23:421
31. Goldfarb I (2005) Phys Rev Lett 95:025501
32. Goldfarb I, Banks-Sills L, Eliasi R (2004) Appl Phys Lett 85:1781
33. Prieto JE, Markov I (2007) Phys Rev Lett 98:176101
34. Okamoto H, Chen D, Yamada T (2002) Phys Rev Lett 89:256101
35. Banin U, Cao YW, Katz D, Millo O (1999) Nature 400:542
36. Steiner D, Aharoni A, Banin U, Millo O (2006) Nano Lett 6:2201
37. Oh J, Meunier V, Ham H, Nemanich RJ (2002) J Appl Phys 92:3332